

Cloud Microphysical and Radiative Properties Derived from MODIS, VIRS, AVHRR, and GMS Data Over the Tropical Western Pacific

*G. D. Nowicki, M. L. Nordeen, P. W. Heck, D. R. Doelling, and M. M. Khaiyer
Analytical Services and Materials, Inc.
Hampton, Virginia*

*P. Minnis
National Aeronautics and Space Administration
Atmospheric Sciences Division
Langley Research Center
Hampton, Virginia*

*S. Sun-Mack
Science Applications International Corporation
Hampton, Virginia*

Introduction

Utilization of the geostationary meteorological satellite (GMS) imagery has allowed for the derivation of cloud and radiative properties over the Tropical Western Pacific (TWP) on relatively high spatial and temporal scales. The layered bispectral threshold method (LBTM) has been applied to GMS data resulting in the ability to study variability and climatological features over a large domain at different spatial scales. The GMS imager only has four channels: visible (VIS; 0.65 μm), infrared (IR; 11- μm), split-window (12 μm), and water vapor (6.7 μm). Without the 3.9- μm channel available on other satellites, it is not possible to derive cloud particle size, water path, and phase accurately and it is difficult accurately determine the heights of optically thin clouds at night. This is an especially important feature over the TWP because thin cirrus clouds constitute a significant portion of the total cloud cover. While the current 3 years of GMS products (available online at <http://www-pm.larc.nasa.gov/arm/TWP/arm-twp.html> and at the ARM Data Center) provide some valuable parameters such as cloud fraction, optical depth (OD), and height and outgoing shortwave (SW) and longwave (LW) fluxes, a more complete characterization of the cloud field is possible using additional spectral channels. Although the ninth Geostationary Operational Environmental Satellite-9 (GOES-9), which carries a 3.9- μm channel, became operational over the TWP during April 2003, there remain more than 4 years of Atmospheric Radiation Measurement (ARM) Program surface-based datasets complemented by only limited satellite data products. To increase the utility of the ARM TWP surface measurements and satellite products and better define the complete diurnal cycle of clouds and the radiation fields, the multi-spectral imager data on the National Oceanic and Atmospheric Administration (NOAA), Earth Observing System (EOS), and Tropical Rainfall Measuring Mission (TRMM) satellites can be analyzed to derive cloud ice and liquid particle sizes, ODs, and water paths as well as improved

cloud heights. Combining the data from these different satellites will provide a better characterization of the cloud fields in the TWP domain than heretofore possible.

Cloud and radiation products are already being derived by the Clouds and Earth's Radiant Energy System (CERES) Project (Wielicki et al. 1998) from the visible infrared scanning radiometer (VIRS) on the precessing-orbit TRMM and from the moderate-resolution imaging spectroradiometer (MODIS) on the Terra and Aqua satellites that have equatorial crossing times of 1030 and 1330 LT, respectively (Minnis et al. 2002b). Similar products can be derived for ARM from advanced very high resolution radiometer (AVHRR) data on the NOAA-14, 15, 16, and 17 satellites that provide sampling at roughly 0600, 0730, 1430, and 0930, respectively. Combining results from all 6 satellites would yield cloud data at up to 12 different local times each day providing an unprecedented look at the large-scale diurnal cycle of clouds over the TWP. Use of multiple satellites to monitor a common set of variables requires careful analysis to ensure consistency between the products determined from the various satellite imagers. This study begins the process of analyzing and comparing AVHRR data to understand differences between the resulting products and similar quantities derived from other satellites. Ultimately, the differences can be taken into account and the AVHRR data can be analyzed on an operational basis to provide a comprehensive cloud dataset over the greater ARM TWP domain.

LBTM Background

Hourly 5-km GMS-5 VIS ($0.63\mu\text{m}$) and IR ($11\mu\text{m}$) radiances, respectively, were analyzed using the LBTM of Minnis et al. (1995) to derive cloud and radiation properties over the TWP domain, currently bounded by 10°N and 10°S latitudes and 130°W and 180° longitudes (Nordeen et al. 2001a). Three predetermined layers, low ($z < 2\text{ km}$), middle ($2\text{ km} \leq z < 6\text{ km}$), and high ($z \leq 6\text{ km}$), are used to classify the cloud properties determined for each grid box and hour. Each pixel is classified as either clear or cloudy. A reflectance model that assumes an effective cloud droplet size of $8\mu\text{m}$ is used to derive OD for low clouds while a hexagonal crystal model representing a cirrostratus size distribution is used to determine OD for midlevel and high clouds. Once OD is known, IR emissivity is calculated and used to adjust cloud-top temperatures for semi-transparent clouds. If the cloud is optically thick, cloud-top temperature and cloud center temperature are equivalent. If OD cannot be calculated, the cloud center temperature is set equal to the IR temperature or, for high clouds, it is set equal to the tropopause temperature and the emissivity and OD are computed. The temperatures are then converted to altitude using vertical profiles of temperature from the European Center for Medium-Range Weather Forecasts (ECMWF) analyses. The ODs and cloud-temperature corrections are not determined at night.

The GMS VIS data were calibrated using the TRMM VIRS as a reference following the approach of Minnis et al. (2002a). Shortwave broadband albedo and outgoing LW flux are derived from the VIS and IR data using narrow-to-broadband conversion functions based on matched 1986 Earth Radiation Budget Experiment (ERBE) and GMS data (Doelling et al. 1996). Albedos and LW fluxes are computed for both clear and cloudy conditions and used to determine the cloud radiative forcing for the period.

The cloud parameters are derived for each pixel and averaged on a $1^{\circ} \times 1^{\circ}$ grid covering the entire TWP domain. The results are also averaged on a $3 \times 3 \times 0.3^{\circ}$ grid covering a domain extending from 0.03°S to

1.02°S and 166.54°E to 167.53°E. The middle box of this smaller grid is centered over Nauru to facilitate comparisons of the satellite results with surface observations. The daytime GMS averages for the 0.9° region centered over Nauru during January, April, July, and October 2001 are used here to compare with the AVHRR results.

VISST Background

The visible infrared solar-infrared split-window technique (VISST) is used to determine cloud properties from satellite images. VISST, a 4-channel model-matching method for plane parallel clouds, uses parameterizations of theoretical radiance calculations for 7 water and 9 ice crystal size distributions and retrieves cloud optical properties by matching calculations to observations (Minnis et al. 2001).

For this study, VISST utilizes the following channels: 0.65 μm (VIS), 3.7 μm (SIR), 10.8 μm (IR), and 12.0 μm (SWC) from 1-km resolution NOAA-14 AVHRR satellite images. The AVHRR VIS channel was calibrated by Doelling et al. (2001) using coincident data from the TRMM VIRS. No changes were made to the nominal SIR, IR, and SWC data. Several additional inputs are required to facilitate satellite retrievals. Atmospheric profiles (1° resolution) derived from ECMWF 6-hourly analyses are used for skin temperature, cloud height calculation, and humidity profiles. Surface type is based on the IGBP 10-minute resolution surface map, remapped to an albedo representation. Clear-sky reflectances and ice and snow masks developed for CERES are used for additional surface characterization (Trepte et al. 1999). Narrowband-to-broadband flux conversion functions, developed from correlations of coincident ERBE-scanner broadband and GOES narrowband fluxes are used to compute broadband SW and LW fluxes from the AVHRR data. AVHRR data within a 1° box centered over Nauru were analyzed for all available daytime overpasses during January, April, July, and October 2001. A single overpass at 0600 Universal Time Coordinates (UTC), January 16, 2001, was also analyzed to test the large-scale robustness of the methodology and to begin the comparisons with CERES-derived products.

Results

A total of 82 matches between the GMS LBTM results and the AVHRR VISST products were found over Nauru for the study period. The maximum time differential of 30 minutes between the GMS and AVHRR images, missing data, and large solar zenith angles (SZA; $>82^\circ$) reduced the number of matches from a potential of nearly 125 points. Most of the SZAs for the matches are between 65° and 75° . Because the VISST and LBTM yield different products, the phase for the LBTM was estimated by assuming that all low clouds were 100% liquid and all high clouds were 100% ice. Mid-level clouds were classified as ice if the mean cloud temperature was <253 K. Otherwise, the midlevel cloud was considered to be a water cloud.

The comparison between the LBTM and VISST results is summarized in Table 1, which shows the mean values of relevant cloud parameters for the entire matched dataset. Except for total cloud heights, the mean values are generally significantly different. The total cloud fraction from AVHRR is 19% less than that from GMS. Ice and water clouds account for 12% and 7% of the total, respectively. The average ODs from AVHRR are nearly twice those from GMS with a greater relative overestimate of the ice cloud ODs. The LBTM yields higher clouds, on average, with the ice cloud heights driving the

difference. The water cloud heights from the VISST exceed those from GMS by 0.6 km, while the ice clouds heights are nearly 2-km less than their GMS counterparts.

Table 1. Mean cloud properties for a 1° region centered on Nauru at the daytime NOAA-14 overpass times during January, April, July, and October 2001 for matched AVHRR and GMS data.		
Cloud Property	AVHRR VISST	GMS-5 LBTM
Total Cloud Amount (%)	50.9	70.1
Ice Cloud Amount (%)	32.2	44.3
Water Cloud Amount (%)	18.6	25.9
Total Optical Depth	5.45	2.95
Ice Optical Depth	5.60	2.25
Water Optical Depth	4.94	2.98
Total Cloud Height (km)	6.2	6.8
Ice Cloud Height (km)	8.5	10.4
Water Cloud Height (km)	3.1	2.5

The discrepancies in these results can be due to a number of factors including differences in resolution, spectral channels, and calibrations and improper thresholds for cloud detection. The higher resolution AVHRR data allows for better discrimination between clear and cloudy pixels than for the 5-km GMS data, especially for the small cloud elements that comprise the cumulus fields typical in the Nauru region. If the cloud fraction is smaller because fewer cloud-contaminated pixels are observed for the same VIS reflectance, then the OD from AVHRR should be greater than its GMS counterpart. Mean ice cloud heights from AVHRR would be lower because the larger ODs produce smaller temperature corrections. Thus, most of the parameter differences are consistent with the cloud amount differences. The water-cloud height differences may be in part due to the somewhat shaky definitions of phase for the LBTM results. Part of the cloud amount difference may be due to the preliminary nature of the AVHRR analyses. It is assumed that the calibrations are correct for all channels and the thresholds and clear-sky backgrounds are the same as expected for the CERES TRMM VIRS analyses. Because of differences in the VIS spectral bands, the VIRS clear-sky reflectances may be different from those for AVHRR. Errors in calibration could also produce similar discrepancies.

The LBTM cloud amounts over Nauru for a different time period were compared with the lidar-derived and the ARSCL (Clothiaux et al. 2000) cloud cover observed directly over the island (Nordeen et al. 2001a). The GMS cloud fraction was nearly equal to the ARSCL cloud amounts, on average, with monthly root mean square differences of 5%. The MPL cloud amounts were roughly 20% less than those from ARSCL. The reasons for the discrepancies are not clear. Nauru produces a distinct island effect on the local cloud cover (Nordeen et al. 2001b) that may influence the surface-satellite comparisons and possibly affect the MPL and ARSCL differences if the MPL and cloud radar, used in the ARSCL, were not collocated. With the uncertainties in the various satellite and surface cloud amounts, further analysis is necessary to determine if the GMS or AVHRR-derived cloud properties need additional refinement.

The large-scale results from AVHRR for 0600 UTC, January 16, 2001, can be compared with those from CERES derived from the TRMM VIRS data taken one half-hour prior to the NOAA-14 overpass. Figure 1 shows the AVHRR cloud mask (Figure 1a) for part of domain (10°N-10°S, 150°E-180°) and the retrieved AVHRR (Figure 1b) and VIRS (Figure 1c) cloud heights for the overpasses, which occurred around 1700 LT. The SZAs for these images ranged from 54° at 10°S, 144°W to 82° at 10°N, 170°W. The location of the VIRS swath is indicated on the AVHRR image. Ice clouds (red) are the predominant cloud type overall with water clouds (blues) being most common in the northeastern part of swath (Figure 1a). The resulting cloud heights from AVHRR range from 1 to 15 km and are generally similar to those from VIRS (Figure 1c) where both analyses yield cloud cover. Some portions of the VIRS image that are covered by clouds are clear in the AVHRR image. In the top of the VIRS height, image, low cloud cover is widespread while few clouds are indicated in the AVHRR result. The water clouds in the center right part of the AVHRR image show significant clear regions in the surrounding areas. The same areas are covered by high clouds in the VIRS retrievals.

Cloud ODs from the two retrievals can be qualitatively compared with the aid of the OD imagery in Figure 2. The ODs from VIRS (Figure 2b) appear to be somewhat greater than the corresponding AVHRR values for OD between 2 and 12, while the AVHRR ODs are larger for the thicker clouds. For the VIRS clouds that are optically thin ($OD < 2$), the corresponding AVHRR pixels have comparable but probably greater values or are classified as clear. Thus, the initial AVHRR algorithm is not detecting many of the optically thin clouds.

Part of the discrepancy can be due to the 30-min time differential. Dying convective systems in some areas could be replaced by developing clouds in other areas. It is unlikely; however, that the large areas of thin cirrus and scattered low clouds detected in the VIRS data would disappear in that short time period. Examination of the VIS imagery (not shown) indicates that reflectances from both satellites exceed 0.2 in the AVHRR clear areas that are identified as cloudy by VIRS, while the reflectances in clear areas common to both retrievals are considerably less than 0.2. Thus, it may be concluded that the initial AVHRR mask is not detecting many of the optically thin clouds, indicating that the GMS results in Table 1 are likely to be more accurate than those from AVHRR. The differences are due either to inaccurate characterization of the clear scenes, errors in the AVHRR calibration, or both.

The comparison of the two retrievals is quantified in Table 2, which lists the mean values of various cloud parameters for the locations common to both datasets. Both ice and water cloud amounts are underestimated by the AVHRR retrieval, while the AVHRR ODs are overestimated, on average. The mean VIRS effective droplet size is 2- μ m larger than the AVHRR values possibly due to the detection of more multilayered clouds with thin cirrus over cumulus. The VIRS water and ice cloud heights also exceed the AVHRR values, a result likely due to a greater semi-transparency correction for the VIRS clouds that have the smaller ODs. The effective cloud ice crystal diameters have virtually the same mean value for both datasets indicating that the 3.7- μ m channel calibrations on both instruments are very similar.

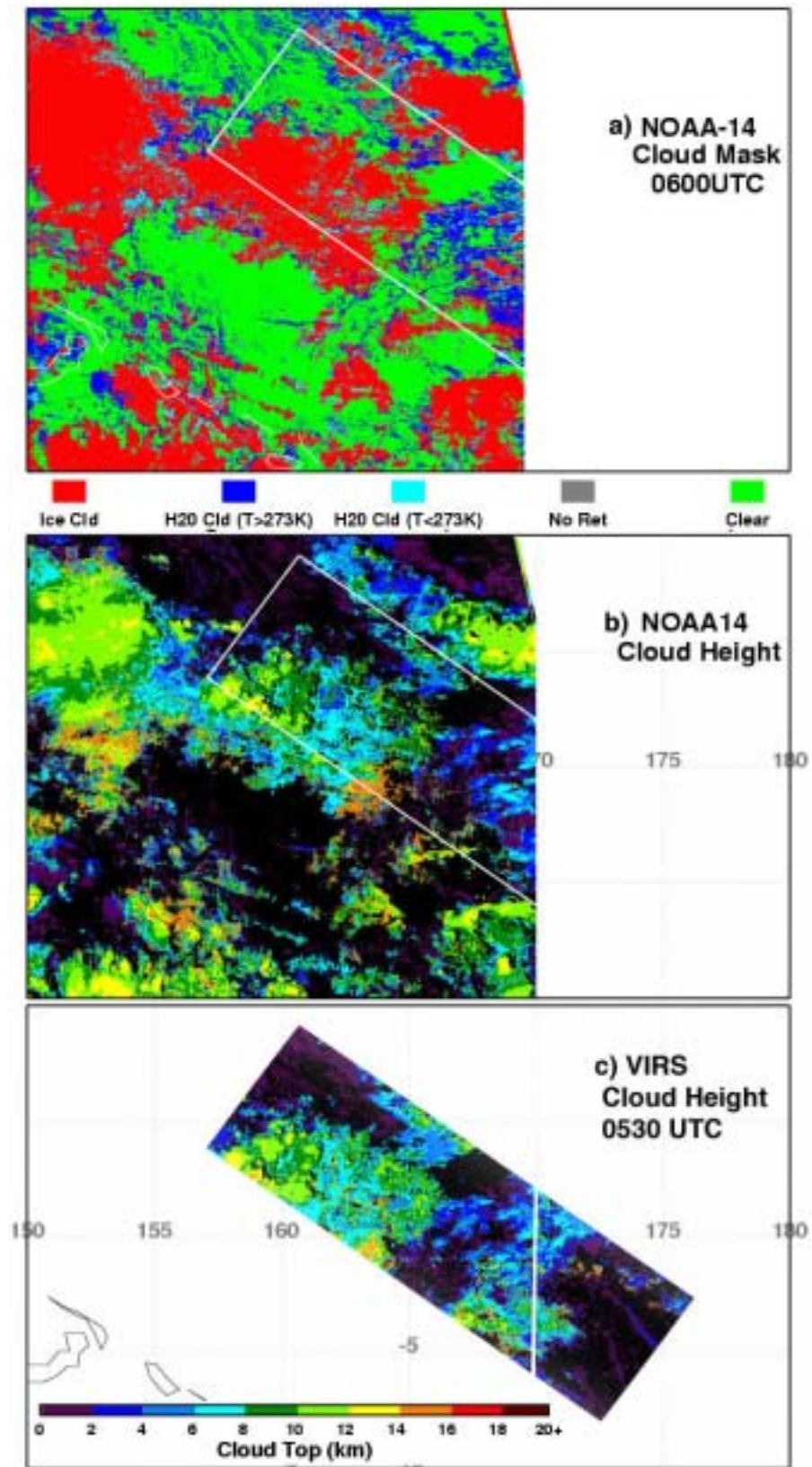


Figure 1. Cloud properties over the TWP (10°N-10°S, 150°E-180°), January 16, 2001.

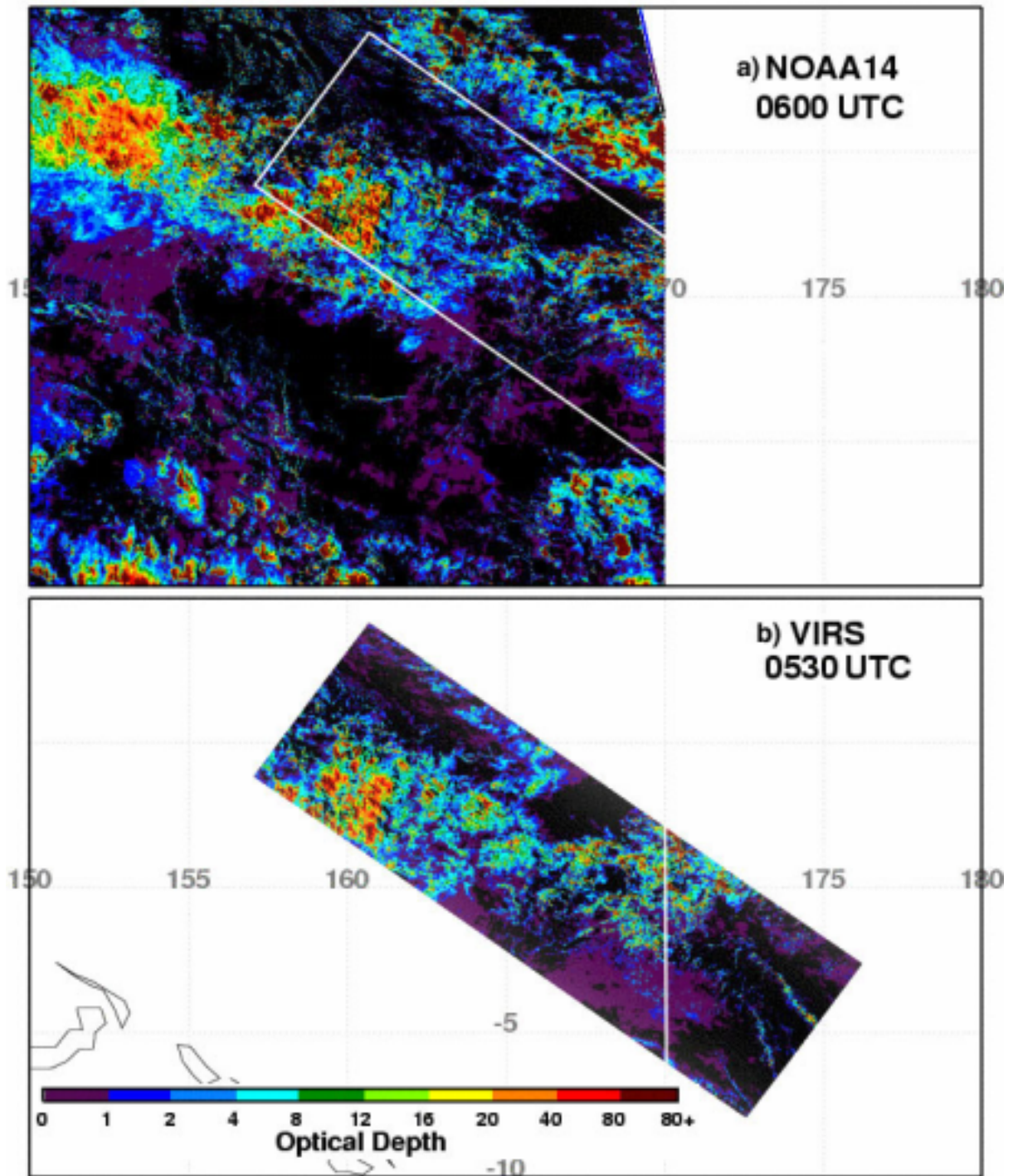


Figure 2. Cloud OD over the TWP (10°N-10°S, 150°E-180°), January 16, 2001.

Table 2. Mean cloud properties for matched AVHRR and VIRS pixels from daytime overpasses during January 16, 2001.			
Cloud Property	AVHRR	VIRS	AVHRR - VIRS
Water cloud amount (%)	25.0	34.7	-9.8
Water OD	2.9	2.4	0.5
Droplet effective radius (μm)	14.8	17.0	2.2
Water cloud height (km)	3.0	3.7	-0.7
Ice cloud amount (%)	41.5	46.7	-5.2
Ice cloud OD	3.2	2.0	1.1
Ice particle eff. diameter (μm)	50.3	51.1	-0.7
Ice cloud height (km)	8.9	9.8	-0.9

Concluding Remarks

The results from a preliminary analysis of AVHRR data over the TWP were compared with data from the ARM TWP GMS analyses and CERES VIRS retrievals. The results suggest some significant errors in either the AVHRR clear-sky characterization or the VIS calibration, or in both. To eliminate these sources of error, the clear-sky albedos and threshold as well as the VIS calibrations will be revisited and adjusted as needed. Additional comparisons with the ARM GMS and CERES VIRS and MODIS results and with similar quantities derived from surface instruments at Nauru, Manus, and Darwin will play a critical role in improving the AVHRR retrievals for all of the NOAA satellites. Because the framework for analyzing the TWP AVHRR data has now been established, it will be possible begin producing AVHRR-based cloud and radiation products when the errors in the AVHRR retrievals have been resolved. GOES-9 began operating over the TWP during April 2003 so that a more complete suite of cloud properties will be derived at high temporal resolution over an expanded domain that will include Darwin, Australia. When the AVHRR and GOES-9 analyses move from the preliminary to the operational stage, the products will be made available on the ARM archive for model validation and better understanding of the interaction between clouds and radiation in the Tropics.

Corresponding Author

Dr. Patrick Minnis, p.minnis@nasa.gov, (757) 864-5671

References

Clothiaux, E. E., T. P. Ackerman, G. G. Mace, K. P. Moran, R. T. Marchand, M. Miller, and B. E. Martner, 2000: Objective determination of cloud heights and radar reflectivities using a combination of active remote sensors at the ARM CART sites. *J. Appl. Meteorol.*, **39**, 645-665.

Doelling, D. R., V. Chakrapani, P. Minnis, and L. Nguyen, 2001: The calibration of NOAA-AVHRR visible radiances with VIRS. *Proc. AMS 11th Conf. Satellite Meteorology and Oceanography*, October 15-18, Madison, Wisconsin, pp. 614-617.

Doelling, D. R., P. Minnis, R. Palikonda, J. K. Ayers, T. P. Ackerman, J. D. Spinhirne, and C. M. R. Platt, 1996: Validation of satellite-derived cloud properties during TOGA/COARE. *12th Intl. Conf. on Clouds and Precipitation Proceedings - Volume 2*, August 19-23, Zurich, Switzerland, pp. 1281-1284.

Minnis, P., W. L. Smith, Jr., D. P. Garber, J. K. Ayers, and D. R. Doelling, August 1995: *Cloud properties derived from GOES-7 for the spring 1994 ARM intensive observing period using Version 1.0.0 of the ARM Satellite Data Analysis Program*, NASA RP 1366, p. 59.

Minnis, P., W. L. Smith, Jr., D. F. Young, L. Nguyen, A. D. Rapp, P. W. Heck, S. Sun-Mack, Q. Trepte, and Y. Chen, 2001: A near-real time method for deriving cloud and radiation properties from satellites for weather and climate studies. *Proc. AMS 11th Conf. Satellite Meteorology and Oceanography*, October 15-18, Madison, Wisconsin, pp. 477-480.

Minnis, P., L. Nguyen, D. R. Doelling, D. F. Young, W. F. Miller, and D. P. Kratz, 2002a: Rapid calibration of operational and research meteorological satellite imagers, Part I: Evaluation of research satellite visible channels as references. *J. Atmos. Oceanic Technol.*, **19**, 1233-1249.

Minnis, P., D. F. Young, B. A. Wielicki, D. P. Kratz, P. W. Heck, S. Sun-Mack, Q. Z. Trepte, Y. Chen, S. L. Gibson, and R. R. Brown, 2002b: Seasonal and diurnal variations of cloud properties derived for CERES from VIRS and MODIS data. *Proc. 11th AMS Conf. Atmos. Rad.*, June 3-7, Ogden, Utah, pp. 20-23.

Nordeen, M. L., D. R. Doelling, P. Minnis, M. M. Khaiyer, A. D. Rapp, and L. Nguyen, 2001a: GMS-5 satellite-derived cloud properties over the tropical western Pacific. In *Proceedings of the Eleventh Atmospheric Radiation Measurement (ARM) Science Team Meeting*, ARM-CONF-2001.

U.S. Department of Energy, Washington, D.C. Available URL:

http://www.arm.gov/docs/documents/technical/conf_0103/nordeen-ml.pdf

Nordeen, M. L., P. Minnis, D. R. Doelling, D. Pethick, and L. Nguyen, 2001b: Satellite observations of cloud plumes generated by Nauru. *Geophys. Res. Lett.*, **28**, 631-634.

Trepte, Q., Y. Chen, S. Sun-Mack, P. Minnis, D. F. Young, B. A. Baum, and P. W. Heck, 1999: Scene identification for the CERES cloud analysis subsystem. *Proc. AMS 10th Conf. Atmos. Rad.*, June 28-July 2, Madison, Wisconsin, pp. 169-172.

Wielicki, B. A., B. R. Barkstrom, B. A. Baum, T. P. Charlock, R. N. Green, D. P. Kratz, R. B. Lee, P. Minnis, G. L. Smith, D. F. Young, R. D. Cess, J. A. Coakley, D. Crommelynck, L. Donner, R. Kandel, M. D. King, A. J. Miller, V. Ramanathan, D. A. Randall, L. L. Stowe, and R. M. Welch, 1998: Clouds and the Earth's Radiant Energy System (CERES): Algorithm Overview. *IEEE Trans. Geosci. Remote Sens.*, **36**, 1127-1141.